Ionization and excitation dynamics of H(1*s*) in short intense laser pulses. II

H. M. Nilsen
Institute of Physics, University of Bergen, Allégaten 55, 5007 Bergen, Norway

L. B. Madsen
Institute of Physics and Astronomy, University of Aarhus, 8000 Århus C, Denmark

J. P. Hansen
Institute of Physics, University of Bergen, Allégaten 55, 5007 Bergen, Norway
(Received 19 April 2002; published 27 August 2002)

In a recent work [J. P. Hansen *et al.*, Phys. Rev. A **64**, 033418 (2001)], we demonstrated that classical methods provide a fair description of excitation and ionization dynamics of H(1*s*) in few-cycle pulses of frequency comparable to the binding energy of the atom and with intensities well below one atomic unit. Here, we extend our studies of classical and quantum dynamics to higher frequencies but similar intensities. For single-cycle pulses with a period smaller than the period of oscillation in the ground state, we observe large differences between quantum and classical physics even in the over-the-barrier regime. As a consequence, care should be exercised when applying classical concepts to the interpretation and understanding of the dynamics of atoms interacting with short pulsed intense lasers in the high-frequency regime.

DOI: 10.1103/PhysRevA.66.025402 PACS number(s): 32.80.Rm, 34.10.+x

Ionization of Rydberg atoms by intense short laser pulses can be accurately described by classical calculations [1]. This result may be seen as an illustration of the correspondence principle stating that predictions of classical and quantum calculations should merge in the limit of high quantum numbers. For ionization from atomic ground states we have no guiding principle, and the question about similarities and/or differences between classical and quantum calculations is more subtle. Recently, this question was addressed in the case of ionization of H(1*s*) [2]. It was found that quantum and classical simulations are in good agreement for pulses with a frequency of $\omega=0.05$ a.u., durations of 5-10 a.u., and for large intensities above the atomic unit of intensity, $I_0=3.51\times10^{16}$ W/cm^2 [atomic units (a.u.) with $e=\hbar=m_e=1$ are used throughout unless indicated otherwise]. Related to the results in [2], and to extensive ionization studies of Geltman [3], we have recently investigated the quantum and classical response of H(1*s*) subject to pulses with frequencies $\omega=0.55$ a.u. and $\omega=0.18$ a.u., corresponding to the one- and three-photon ionization regimes [4]. Our field amplitudes E_0 were smaller or equal to 0.33 a.u. and the pulse lengths were varied from 10 a.u. to 5×10^2 a.u. We showed that results based on classical trajectory Monte Carlo (CTMC) simulations were capable of explaining the main features of the dynamics induced by the electromagnetic pulse. For differential quantities such as the photoelectron spectrum and the angular distribution of the ionized electron, the classical predictions were of lower quantitative quality, but still in satisfactory qualitative agreement with the quantum predictions. In particular, classical simulations allowed us to understand the ionization dynamics in terms of electron cloud oscillations following the electromagnetic field: Excitation, propagation, rescattering, and ionization. We also showed that classical dynamics in the three-photon ionization regime was in a less good agreement with the quantum results than the corresponding results in the one-photon regime. This was attributed to the quantized nature of the light field being more pronounced for lower frequencies. We note in passing that in parallel to the quantum and classical studies, semiclassical methods have been used with success to describe strong-field laser-atom interactions (see, e.g., Ref. [5], and references therein).

In this work we extend our studies to the regime of higher frequencies, and we investigate to what extent one can apply classical pictures as well as classical methods to describe the ionization process for few-cycle high-frequency pulses. This is done primarily to address the fundamental question of classical and quantum correspondences. Such studies might very well prove to be experimentally feasible in the future since femtosecond intense laser pulses containing only a few optical cycles were recently demonstrated in several laboratories for visible light [6–9], and very recently even the generation of attosecond pulses of soft x-ray radiation was achieved [10].

In this Brief Report brief summaries of the theoretical approaches for the classical and quantum calculations are given. Details were presented in Ref. [4]. We consider a H(1*s*) atom exposed to a linearly polarized time-dependent electric field described by the following form:

$$\vec{E}(t)=E_0\sin^2(t\pi/T)\cos(\omega t+\phi)\vec{e}_z, \quad 0<t<T, \qquad (1)$$

where E_0, T, and $\vec{e}_z$ are the amplitude, pulse duration, and the polarization vector, respectively. The temporal part of the pulse envelope is described by the $\sin^2$ function. To ensure a pulse without unphysical dc components, we choose the phase ϕ such that the vector potential $\vec{A}(t)=-\int_0^t\vec{E}(t')dt'$ is zero for $t>T$ [11].

In our quantum mechanical formulation, the time-dependent Schrödinger equation is solved by expanding the wave function in a basis spanning a large number of bound states and discretized continuum states,

$$\Psi(\vec{r},t)\approx\sum_{n=1}^{n_{\max}}\sum_{l=0}^{n-1}a_{n,l}(t)R_{n,l}(r)Y_{l,m=0}(\hat{r}) + \sum_{k_i=1}^{k_{\max}}\sum_{l=0}^{l_{\max}}b_{k_i,l}(t)\Phi_{k_i,l}(r)Y_{l,m=0}(\hat{r}). \quad (2)$$

The coefficients $a_{n,l}(t)$ and $b_{k_i,l}(t)$ are the amplitudes for bound and continuum states, respectively. Calculations where the Schrödinger equation is solved directly by a grid method [12] are also performed with identical results. The angle integrated photoelectron spectrum is given in terms of the probabilities of the continuum functions

$$\frac{dP}{dE_i}=\sum_{l=0}^{L_{\max}}|b_{k_i,l}(T)|^2, \quad E_i=k_i^2/2, \quad (3)$$

and the angular distribution is obtained by

$$\frac{dP}{d\theta}\propto\sum_{k_i}\left|\sum_{l}(-i)^l b_{k_i,l}(T)e^{i\sigma_l}Y_{l,0}(\theta)\right|^2, \quad (4)$$

where σ_l is the Coulomb phase shift. At the most detailed level, we consider the time development of the spatial probability density given by $\rho_{QM}(x,y,z,t)=|\Psi(\vec{r},t)|^2$. Due to rotational symmetry a cut for $y=0$ carries all information about ρ_{QM} at a given time.

The classical trajectory Monte Carlo (CTMC) calculations are based on the solution of classical equations of motion for a large number of trajectories ($N=10^6$). Each trajectory corresponds to an initial condition picked at random from a microcanonical ensemble [13]. To compare with the quantum mechanical probability density, ρ_{QM}, we calculate the classical density by $\rho_{CL}(r_j,z_i;t)=(1/V_{i,j})\,(N_{i,j}/N)$, where N is the total number of initial conditions in the ensemble, $N_{i,j}$ is the number of trajectories at time t in the cylindrical region of configuration space given by $z_i-dz\leq z<z_i+dz$, $r_j-dr\leq r<r_j+dr$, $r=\sqrt{x^2+y^2}$, and where $V_{i,j}=8\pi r_j dr dz$ is the corresponding volume.

The energy and the angular distributions are straightforwardly obtained by binning events into differential reaction windows, and in this way building up a histogram. Note that the events for the angular distribution of the ionized electron should be binned at electronic distances sufficiently far from the nucleus to ensure straight line paths.

Our quantum and classical calculations are performed for a pulse about one cycle long, with a frequency $\omega=1.4$, amplitude $E_0=0.333$, pulse length $T=6.0$, and phase $\phi=0.5124$ [see Eq. (1)]. The electrical field as a function of time is shown in Fig. 1.

In Fig. 2 we show the energy distribution of the ionized electrons. A clear difference between quantum and classical results is seen. The total quantum ionization probability is twice that of the classical case, and in the photoelectron energy spectrum, we observe a pronounced cutoff in the classical result absent in the quantum mechanical case. For the angular distribution, Fig. 3, we also observe a startling difference between the classical and quantum mechanical pictures. The classical result is peaked in one direction, while in the quantum mechanical case, the distribution has the characteristic *p*-wave shape of one-photon ionization from an initial *s* state. Figure 4 displays the probability distribution of the continuum for the quantum calculations. The corresponding CTMC picture is shown in Fig. 5. From studying Fig. 3 and comparing Figs. 4 and 5, again we note the presence of the characteristic *p*-wave shape in the quantum mechanical case, and its absence in the classical case.

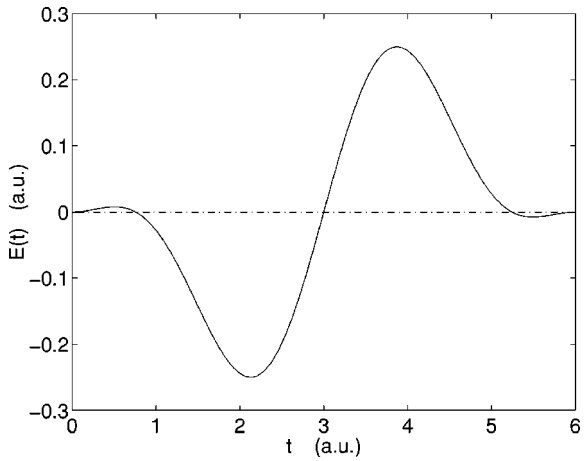

FIG. 1. Time-dependent electric field experienced by the atom. $E_0=0.333$, $\omega=1.4$, $T=6.0$, and $\phi=0.5124$ in Eq. (1).

To understand the classical mechanism of ionization, we plot, in Fig. 6, the initial distribution of the electrons which ionize classically. From Fig. 6 it is clear that all the ionizing trajectories come from the same volume of configuration space. Classically, the ionization process takes place for electrons which have their velocity in the same direction as the force of the perturbing field, and therefore can absorb enough energy to ionize. We see that the electrons which ionize in the CTMC calculation are the electrons which start from the negative z position of Fig. 6 and would have ended about there even without the field. Hence, in this regime, the classical ionization involves a strong resonance-like synchroni-

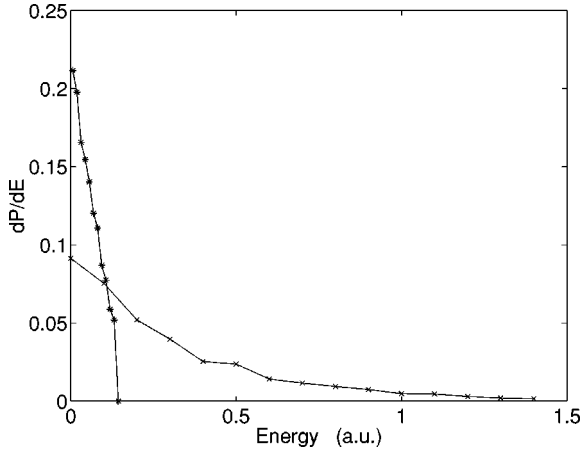

FIG. 2. Normalized photoelectron energy spectrum as given by Eq. (3) for the pulse in Fig. 1. $-\times-\times-\times-$ for quantum calculations and $-*-*-*-$ for classical calculations. The total quantum (classical) ionization probability is ~ 0.04 (~ 0.02).

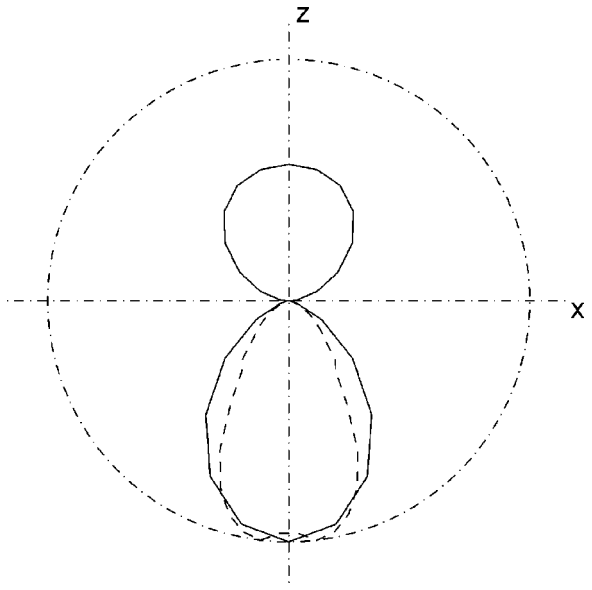

FIG. 3. Angular distributions as given by Eq. (4) for the pulse shown in Fig. 1. Solid line indicates quantum calculations and dashed line for classical calculations. The forward direction is marked with "z" (polar angle 0°) and the perpendicular direction by "x" (polar angle 90°).

zation between the field-free motion and electronic motion induced by the perturbing field. The effect of the field is that it only transfers energy effectively to the electron along specific resonant trajectories, and only in these cases forces it to ionize. In the quantum mechanical case, the situation is different, as illustrated by the fact that the *p*-wave character of the wave function is recognized. From a matrix element consideration, the *p*-wave is the only first order contribution for ionization from the initial *s* state. That is, we will get probabilities in both directions as long as no other angular momentum states are populated. Interactive movies of the classical and quantum probability distribution are available on the World Wide Web [14].

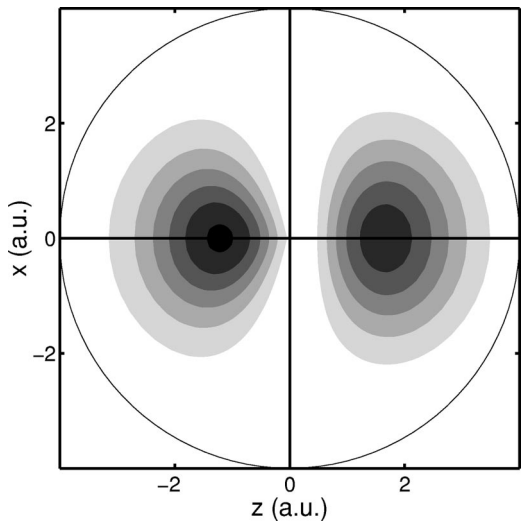

FIG. 4. The spatial quantum mechanical probability density, $\rho_{QM}(x,y=0,z,t=T)$, for positive energy electrons at the end of the pulse of Fig. 1.

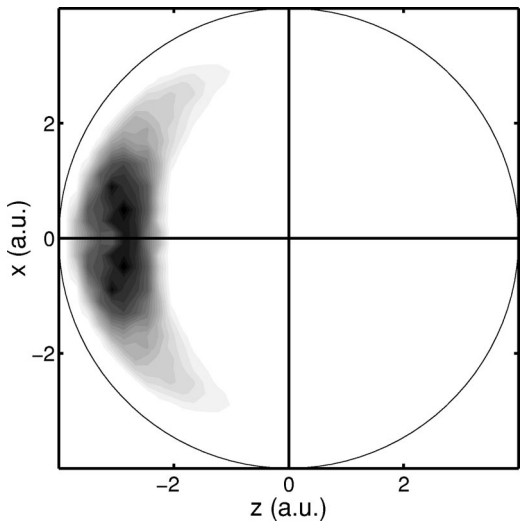

FIG. 5. The spatial CTMC probability density, $\rho_{CL}(x,y=0,z,t=T)$, for positive energy electrons at the end of the pulse of Fig. 1.

Our calculations illustrate that for short pulses, the electrons which acquire most energy classically come from a localized volume. In the quantum case such a localized wave packet would quickly spread out due to dispersion. A wave packet in free space will disperse with a speed $(1/\Delta x)$, where Δx is the width of the initial wave packet considered. This means that a wave packet corresponding to Fig. 6 would have smeared out to about ~ 6 a.u. in the *z* direction during the pulse. This illustrates the failure of considering this system classically. The reason for the discrepancy between quantum and classical methods is that we are in a regime where the classical contributions to ionization come from trajectories which fulfill a resonance condition with the field. Quantum mechanically such "trajectory-resonances" stemming from strongly localized volumes in phase space will be blurred due to quantum pressure, and in the quantum mechanical case the process is dominated by resonant perturbative *s* to *p* ionization.

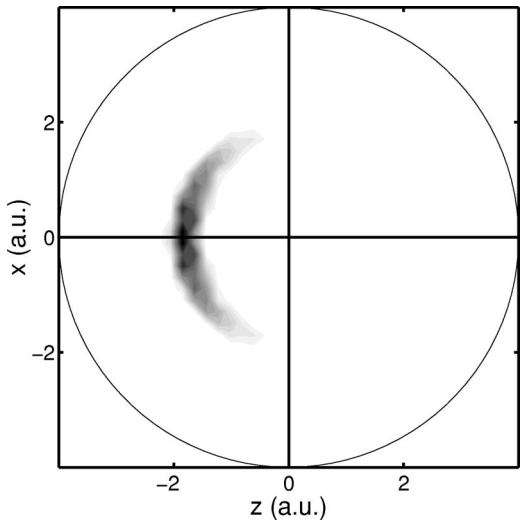

FIG. 6. The spatial CTMC probability density as a cut in the *x*-*z* plane for the initial conditions which ionize classically.

In summary, we have extended our classical and quantum studies [4] of atom–few-cycle-laser pulse interactions to higher frequencies. Here and in Ref. [4] we have considered field strengths below 1 a.u., and specifically we have worked with $E_0 = 0.333$ a.u. In [4], we found good agreement in the one-photon ionization regime ($\omega = 0.55$) and a poorer agreement in the three-photon ionization regime ($\omega = 0.18$). In this work, we have reported pronounced differences between the classical and quantum mechanical results at high frequency, $\omega = 1.4$. These studies show that if the external field introduces a really strong perturbation of short duration as is the case for $\omega = 0.55$, classical predictions will do fine, but if the processes involved take place with smaller perturbative-like probabilities, the quantum nature of the atom becomes important. In particular, classical calculations and pictures can be completely unsuitable for describing ionization in a laser pulse of short duration when the laser frequency becomes large.

This research was supported by the Norwegian Research Council (H.M.N.) and by EU Project Nos. HPRI-CT-1999-00094 and HPMFCT-2000-00686. L.B.M. is supported by the Danish Natural Science Research Council (Grant No. 51-00-0569).

[1] F. Robicheaux, Phys. Rev. A **56**, R3358 (1997); **60**, 431 (1999).
[2] G. Duchateau, E. Cormier, and R. Gayet, Eur. Phys. J. D **11**, 1991 (2000); G. Duchateau, C. Illescas, B. Pons, E. Cormier, and R. Gayet, J. Phys. B **33**, L571 (2000); G. Duchateau, E. Cormier, H. Bachau, and R. Gayet, Phys. Rev. A **63**, 053411 (2001).
[3] S. Geltman, J. Phys. B **33**, 1967 (2000).
[4] J.P. Hansen, J. Lu, L.B. Madsen, and H.M. Nilsen, Phys. Rev. A **64**, 033418 (2001).
[5] G. van de Sand and J.M. Rost, Phys. Rev. A **62**, 053403 (2000).
[6] A. Baltuska, Z. Wei, M.S. Pshenichnikov, D.A. Wiersma, and R. Szipöcs, Appl. Phys. B: Lasers Opt. **65**, 175 (1997).
[7] L. Gallmann, D.H. Sutter, N. Matuschek, G. Steinmeyer, U. Keller, C. Iaconis, and I.A. Walmsley, Opt. Lett. **24**, 1314 (1999).
[8] U. Morgner, F.X. Kärtner, S.H. Cho, Y. Chen, H.A. Haus, J.G. Fujimoto, E.P. Ippen, V. Scheuer, G. Angelow, and T. Tschudi, Opt. Lett. **24**, 411 (1999).
[9] M. Nisoli, S. Stagira, S. De Silvestri, O. Svelto, S. Sartania, Z. Cheng, M. Lenzner, C. Spielmann, and F. Krausz, Appl. Phys. B: Lasers Opt. **65**, 189 (1997).
[10] M. Hentschel, R. Kienberger, Ch. Spielmann, G.A Reider, N. Milosevic, T. Brabec, P. Corkum, U. Heinzmann, M. Drescher, and F. Krausz, Nature (London) **414**, 509 (2001).
[11] L.B. Madsen, Phys. Rev. A **65**, 053417 (2001).
[12] M.R. Hermann and J.A. Fleck, Jr., Phys. Rev. A **38**, 6000 (1988).
[13] C.O. Reinhold, M. Melles, and J. Burgdörfer, Phys. Rev. Lett. **70**, 4026 (1993); C.O. Reinhold *et al.*, J. Phys. B **26**, L659 (1993).
[14] http://www.fi.uib.no/~nilsen/movies/shortpulsmovie.html